

ORBITAL PERTURBATION

Winter Project, 2022





MEMBERS

ADIT JAIN

ATHARVA DEHADRAYA

SHASHANK SINHA

SHASHANK RAPOLU

VASU PALIWAL

YASHIKA MALHOTRA

Orbital Perturbations

Contents

1	Introduction	4
2	Reasons for Perturbations	4
3	Mathematics	4
3.1	Setting up the system	4
3.2	Calculating \dot{a}	5
3.3	Calculating \dot{e}	5
3.4	Calculating \dot{i}	5
3.5	Calculating $\dot{\Omega}$	5
3.6	Calculating $\dot{\omega}$	5
4	Drag Perturbations	5
4.1	Calculation	5
4.2	Estimation of Ballistic Coefficients	5
4.3	Effect	6
4.4	Countering the effects	6
5	Non-Spherical Earth	6
5.1	Measurement of the potential field of the earth	7
5.1.1	LAGEOS (Laser Geodynamics Satellites)	7
5.1.2	GRACE	7
5.2	Potential Equation	7
5.2.1	Zonal Harmonics	7
5.2.2	Sectorial Harmonics	8
5.2.3	Tesseral Harmonics	8
5.3	The J2 Perturbation	8
5.4	J2 Effect	9
5.5	J2 Special Orbits	10
6	Positive Perturbations	10
6.1	Lift and Slow Landing	10
6.2	Debris Management	10
6.2.1	Graveyard Orbits	10
6.2.2	Disposal Orbits	10
6.3	Lower ΔV requirement/ Gravity Assist	11
6.3.1	Using Lunar Gravity	11
6.3.2	Interplanetary Superhighway	11
6.4	Asteroid Protection	11
6.4.1	Natural	11
6.4.2	Artificial	11
7	Newton's n-body problem	11
7.1	What it is?	11
7.2	Derivation of equations	11
7.3	3-Body problem	12
7.4	Chaos Theory	12
7.5	Lagrange Points	12
8	Case Study: James Webb Space Telescope	13
8.1	Introduction	13
8.2	Positioning at L2	13
8.3	Interesting Facts	13

1. Introduction

Spacecraft control and maneuver as well as accurate mapping of trajectories of asteroids require precision tracking of their movement in space. While their orbits can be calculated relatively easily by only considering the major forces being applied on the body, over time the minor forces build up resulting in a completely different orbit.

Hence, in order to accurately predict their movement, these "perturbations" need to be taken into account as well. Perturbations can cause both positive and negative effects.

2. Reasons for Perturbations

Perturbations might be caused due to various phenomenon, both natural as well as man-made. Here, are some of the major reasons for perturbations:

- Atmospheric Drag
- Neglected gravitational forces
- Non-Spherical shape of the Earth
- Collision with Space Debris

Let start off by constructing a new co-ordinate system in order to make it easier to calculate various forces acting on a body.

3. Mathematics

Firstly, we define a new coordinate system as shown in the figure given below:

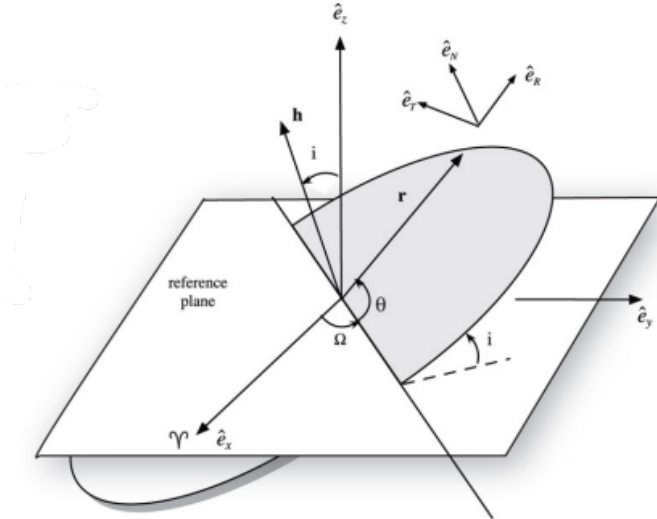


Fig-1: Satellite Normal Coordinate System

For the rest of the paper, we'll refer to it as the Satellite-Normal coordinate system. Here, we have assumed the orbit of the satellite to be an ellipse with the earth at one of the focii.

3.1. Setting up the system

The 3 perpendicular vectors are defined as follows:

- \hat{e}_R points along the earth: satellite vector
- \hat{e}_N points in the direction of \vec{h} i.e. the angular momentum of the satellite about the center of the earth

- \hat{e}_T points in the direction of $\hat{e}_N \times \hat{e}_R$

A general force on the satellite in this coordinate system can then be written as:

$$\vec{F} = N\hat{e}_N + R\hat{e}_R + T\hat{e}_T \quad (1)$$

Where N, R, T are completely arbitrary variables.

But due to perturbations, some of the quantities that we earlier assumed to be constant are now varying. For example: (Earth's coordinate system $[\hat{x}, \hat{y}, \hat{z}]$ is assumed to be fixed)

- a = semi-major axis of the ellipse of the satellite
- e = eccentricity of the ellipse of the satellite
- i = Inclination = angle between angular momentum of the satellite and earth's normal
- Ω = Right Ascension of the Ascending Node, a.k.a. RAAN
- ω = argument of perigee

Hence, to find them out, we need to find out their derivatives, most of which depend upon \vec{h} (angular momentum) and E (total energy):

$$a = -\frac{\mu}{2E} \quad (2)$$

$$e = \sqrt{1 + \frac{2Eh^2}{\mu^2}} \quad (3)$$

$$\cos i = \frac{h_z}{h} \quad (4)$$

$$\tan \Omega = -\frac{h_x}{h_y} \quad (5)$$

where, $\mu = GM_E M_S$, the natural convention. Note that here we have assumed energy and momentum loss due to perturbations. Hence, E and \vec{h} are assumed to be varying and consequently, a quasi-static elliptic path of the satellite. Hence, we are focusing more on the derivatives of the above variables.

Hence, we first need to find out $\dot{\vec{h}}$ and \dot{E} . Now, the general force, \vec{F} , acting on the satellite at the radial position, \vec{r} can be written as:

$$\vec{F} = \begin{bmatrix} N \\ R \\ T \end{bmatrix}, \quad \vec{r} = \begin{bmatrix} r \\ 0 \\ 0 \end{bmatrix}$$

Energy

$$\begin{aligned} \dot{E} &= \frac{d}{dt} \vec{F} \cdot \vec{dr} \\ &= \vec{F} \cdot \frac{d\vec{r}}{dt} \\ &= \vec{F} \cdot \vec{v} \\ &= \vec{F} \cdot (r\hat{e}_R + r\dot{\theta}\hat{e}_T) \\ &= \dot{r}r + r\dot{\theta}T \end{aligned} \quad (6)$$

Angular Momentum

$$\begin{aligned} \dot{h} &= |\vec{r} \times \vec{F}| \\ &= |rT\hat{e}_N + rN\hat{e}_T| \\ &= \frac{\vec{h} \cdot \dot{\vec{h}}}{|h|} \\ &= \frac{(h\hat{e}_N) \cdot (rT\hat{e}_N - rN\hat{e}_T)}{|h|} \\ &= rT \end{aligned} \quad (7)$$

Now onto calculating $\dot{\theta}$ and \dot{r} :

$$\dot{\theta} = \frac{d}{dt}(\omega + f) \cong \dot{f} = \frac{h}{r^2}$$

By definition,

$$h = r \cdot v_{\perp} = r(\dot{r}\dot{f}) = r^2\dot{f}$$

$$r = \frac{h^2/\mu}{1 + e \cos f} \Rightarrow \dot{r} = \frac{\dot{f}er^2 \sin f}{h^2/\mu} = \frac{\mu e \sin f}{h}$$

3.2. Calculating \dot{a}

Now, on differentiating a w.r.t time to obtain \dot{a} , we get,

$$\dot{a} = \frac{da}{dE} \frac{dE}{dt} = \frac{\mu}{2E^2} \dot{E}, \quad ... E = -\frac{\mu}{2a}$$

$$\Rightarrow \dot{a} = 2 \frac{a}{\mu^2} \left(R \frac{\mu e \sin f}{h} + T \frac{h}{r} \right)$$

$$\Rightarrow \dot{a} = 2 \sqrt{\frac{a^3}{\mu(1-e^2)}} [eR \sin f + T(1 + e \cos f)] \quad (11)$$

3.3. Calculating \dot{e}

Now, on differentiating e w.r.t time to obtain \dot{e} , we get,

$$\dot{e} = \frac{1}{2e} (e^2 - 1) \left(2 \frac{\dot{h}}{h} - \frac{\dot{E}}{E} \right) \quad (12)$$

$$\Rightarrow \dot{e} = \sqrt{\frac{a(1-e^2)}{\mu}} [R \sin f + T(\cos f + \cos E_{ecc})] \quad (13)$$

where E_{ecc} is the eccentric anomaly, defined as:

$$\tan\left(\frac{E_{ecc}}{2}\right) = \sqrt{\frac{1-e}{1+e}} \tan\left(\frac{f}{2}\right) \quad (14)$$

And, r was rewritten as:

$$r = a(1 - e \cos E_{ecc})$$

3.4. Calculating \dot{i}

Now, on differentiating $\cos i$ (Angle of inclination) w.r.t time to obtain \dot{i} , we get,

$$\cos i = \frac{h_z}{h}$$

$$\Rightarrow \frac{d}{dt} i = \frac{1}{\sin i} \frac{hh_z' + hh_z}{h^2}$$

$$= \sqrt{\frac{a(1-e^2)}{\mu}} \left(\frac{N \cos(w+f)}{1+e \cos f} \right) \quad (15)$$

3.5. Calculating $\dot{\Omega}$

(8) Now, on differentiating $\tan \Omega$ (RAAN) w.r.t time to obtain $\dot{\Omega}$, we get,

$$\tan \Omega = -\frac{h_x}{h_y}$$

$$\Rightarrow \frac{d}{dt} \Omega = \frac{h_x h_y' - h_x' h_y}{h_y^2} \cos^2(\Omega)$$

$$= \sqrt{\frac{a(1-e^2)}{\mu}} \left(\frac{N \sin(w+f)}{(1+e \cos f) \sin(i)} \right) \quad (16)$$

3.6. Calculating $\dot{\omega}$

Similarly, $\dot{\omega}$ can also be calculated as shown:

$$\dot{\omega} = -\Omega \cos i + \sqrt{\frac{a(1-e^2)}{e^2 \mu}} \left(-R \cos f + T \frac{(2+e \cos f) \sin f}{(a+e \cos f)} \right) \quad (17)$$

4. Drag Perturbations

4.1. Calculation

As was derived in the Summer Project, 2021 - [Space: The Final Frontier](#), we calculated the drag force on rockets, which incidentally can be applied to satellites to a great extent:

$$F_D = C_D Q A = \frac{1}{2} \rho v^2 C_D A \quad (18)$$

where

- Q = Dynamic pressure
- A = Area of satellite projected onto the $\hat{e}_N - \hat{e}_R$ plane
- C_D = Coefficient of drag

We can also define another variable, B , known as the Ballistic Coefficient as follows:

$$B = \frac{m}{C_D A} \quad (19)$$

Then, the force on the satellite due to drag can be written in the form of eq. 1 as:

$$N = R = 0, \quad T = -\frac{1}{2} \frac{\rho}{m} C_D A v^2 = -\frac{1}{2} \frac{\rho v}{B} \quad (20)$$

4.2. Estimation of Ballistic Coefficients

For space objects with perigee altitude below 600 km, the variation in the semi-major axis is mainly caused by drag perturbation. Therefore, the ballistic coefficients can be estimated based on variation of mean semi-major axis derived from the TLEs (Two Line Element).

The variation in mean semi-major axis primarily comes from atmospheric drag. The atmospheric drag on an object will continually decrease the osculating semi-major axis a , according to:

$$\frac{da}{dt} = \frac{2a^2 v}{\mu} \dot{v}_d \cdot e_v \quad (21)$$

where

- μ = Product of gravitational constant and mass of earth
- v = Speed of the object
- e_v = Unit vector in the direction of v
- \dot{v}_d = Acceleration of object due to drag

$$\dot{v}_d = -\frac{1}{2}\rho BC |v - V|^2 e_{v-V} \quad (22)$$

where

- V = Atmospheric wind velocity vector
- e_{v-V} = Unit vector of the object's motion relative to the atmospheric wind.

The rate of change of mean semi-major axis due to atmospheric drag is given by:

$$\frac{da_d}{dt} = -a_m^2 \mu^{-1} \rho BC v^3 F \quad (23)$$

where a_m is the mean semi-major axis and the dimensionless wind factor F is given by

$$F = \frac{|v - V|^2}{v} e_{v-V} \cdot e_v \quad (24)$$

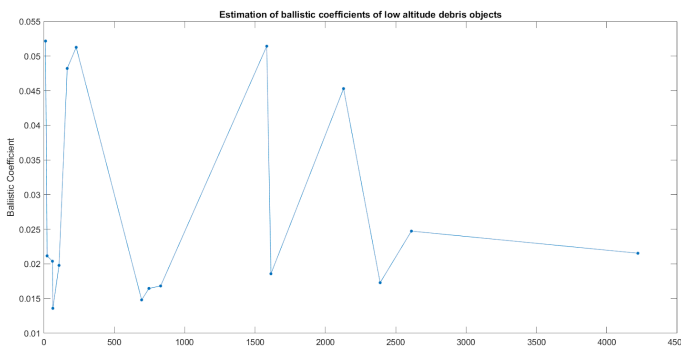
Integrating equation (23) from t_1 to t_2 , we get:

$$\Delta_{t_1}^{t_2} a_d = -\mu \sum_{t=t_1}^{t=t_2} a_m^2 \rho BC v^3 F \Delta t \quad (25)$$

where Δt is the time step for numerical integration. Thus, the BC can be computed by:

$$BC = -\frac{\mu \Delta_{t_1}^{t_2} a_d}{\sum_{t=t_1}^{t=t_2} a_m^2 \rho v^3 F \Delta t} \quad (26)$$

The following plot shows the variation of ballistic coefficients with NORAD ID of the satellite



4.3. Effect

Assuming circular orbit motion of the satellite in a uniform density atmosphere, we can conclude the following effects:

Since $N=0$, the orbital plane doesn't change, so,

1. $\dot{\Omega} = 0$
2. $\frac{d}{dt} i = 0$

Effect on semi-major axis, or, radius in this case:

Since $e=0$, from eq. 11,

$$\dot{a} = -\sqrt{\frac{a^3}{\mu}} \frac{\rho}{m} C_D A v^2 = -\sqrt{\frac{a^3}{\mu}} \frac{\mu^2}{a^2} \frac{\rho}{B} = -\sqrt{a \mu} \rho B \quad (27)$$

Integrating this equation w.r.t. time, we obtain:

$$a(t) = \left(\sqrt{a(0)} - \sqrt{\mu} \frac{\rho}{B} t \right)^2 \quad (28)$$

But in the real world, the atmospheric density is rarely constant and varies with time, $\rho(t)$. This is primarily due to two factors as follows:

Exponential Growth Since \vec{r} varies with time, we can also write $\rho(r)$. As we come closer to earth's surface, the density begins to grow exponentially.

Solar Activity Unpredictable solar activity, like solar wind may effect the atmospheric composition, especially in the ionosphere while simultaneously changing the earth's EM field.

Secondly, the orbits of the satellites are almost always eccentric. Eccentric orbits are particularly prone to drag. If e is very small and a is sufficiently high, we can assume that the majority of the drag effects will occur near and at perigee. Consequently, the apogee height will decrease with time, which will be quite significant. The resulting equations are extremely complicated and difficult to integrate and hence, an Exponential Decay model is used to calculate Δe

4.4. Countering the effects

Drag will inadvertently lead to loss of velocity, so we need the satellite to have enough Δv (m/s/year) to counteract the effects of drag and maintain it's orbit. This is also known as Δv budgeting.

Despite accurate models, we are unable to decide the precise Δv budget due to the unpredictable pattern of solar winds.

Highly efficient maneuvers are done to gain the Δv lost to drag. This is known as station-keeping. Since there is only a limited amount of fuel available to the satellite, it's orbit will eventually decay, bringing it's life to an end by burning up in the atmosphere. The "lifetime" of a satellite is defined by the time it takes to cross the Kármán Line (100 km).

5. Non-Spherical Earth

So far we have considered earth as a perfectly spherical homogeneous body but earth neither has a homogeneous mass distribution nor is a spherical body. Consequently, the several attributes of the Earth's shape and composition have noticeable affects on a satellite's orbit around earth and therefore cannot be neglected.

For a spherical earth, dU is symmetric

$$dU = -\frac{2\pi R^2 G \sigma m_2 \sin\theta}{\rho} d\theta \quad (29)$$

The actual gravity is not precisely spherical as density varies throughout the earth. The result is a distorted potential field (**geoid**) as shown below.

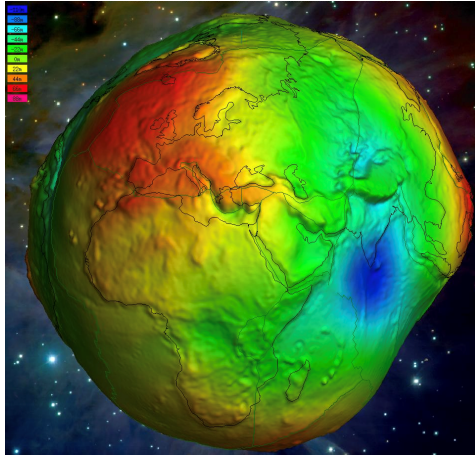


Fig-2: Earth's Potential Field

5.1. Measurement of the potential field of the earth

Different methods and computational techniques have been invented in due time to reflect various types of input gravity or gravitational gradient data. Initially, the geoid determination relied on surface gravity data defined as first-order gravity gradients. Second-order gravity gradients are measurable at the land surface by the torsion balance. In the new millennium, several gravity-dedicated satellite missions have already been realized.

5.1.1. LAGEOS (Laser Geodynamics Satellites)

Precisely measuring the trajectory of a satellite as it orbits the earth then accounting for drag, third-body dynamics, etc. and remaining perturbation must be caused by gravitational potential. The orbits of the *LAGEOS* satellites are measured precisely by laser reflection.



Fig-3: LAGEOS Satellite

5.1.2. GRACE

Measuring satellites position from earth is inaccurate so the GRACE project measures the relative position of two adjacent satellites. Relative motion yields gradient of the potential field and direct construction of $U(\vec{r})$ can be made.

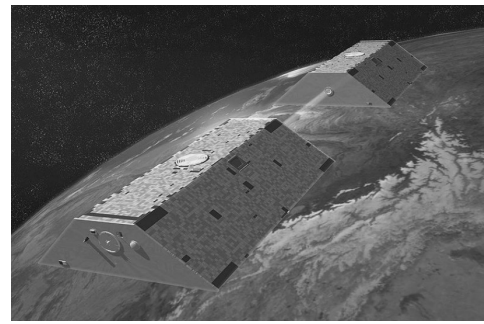


Fig-4: GRACE Satellite

5.2. Potential Equation

The potential has the form:

$$U(\phi_{gc}, \lambda, r) = \frac{\mu}{r} + U_{zonal}(r, \phi_{gc}) + U_{oblat}(r, \lambda) + U_{perturb}(r, \phi_{gc}, \lambda) \quad (30)$$

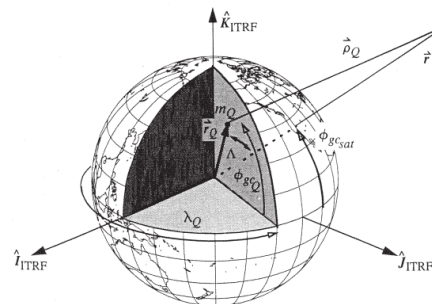


Fig-5: Earth's Potential Coordinate System

where

- ϕ_{gc} = declination from equatorial plane
- λ = right ascension, measured from Greenwich meridian
- r = radius

5.2.1. Zonal Harmonics

The zonal spherical harmonics are special spherical harmonics that are invariant under the rotation through a particular fixed axis. They only vary with latitude. These have the form:

$$U_{zonal}(r, \phi_{gc}) = \frac{\mu}{r} \sum_{i=2}^{\infty} J_i \left(\frac{R_e}{r} \right)^i P_i(\sin(\phi_{gc})) \quad (31)$$

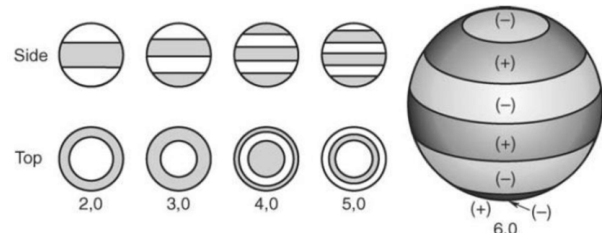


Fig-6: Zonal Harmonics

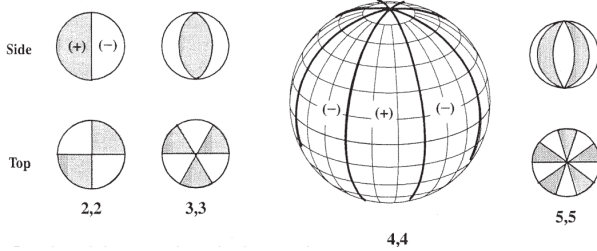
where

- R_e is the earth radius
- P_i are the Legendre Polynomials
- The J_i are determined by the Geodesy data

5.2.2. Sectorial Harmonics

These have the form:

$$U_{sectorial}(r, \lambda) = \frac{\mu}{r} \sum_{i=2}^{\infty} (C_{i,sect} \cos(i\lambda) + S_{i,sect} \sin(i\lambda)) \left(\frac{R_e}{r}\right)^i P_i(\sin \phi_{gc}) \quad (32)$$

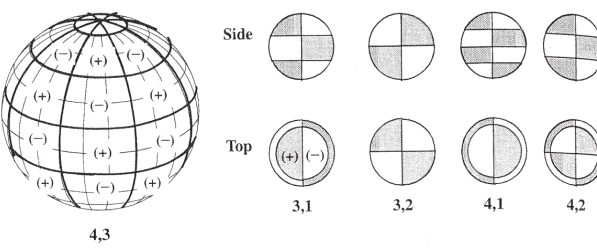


where, $C_{i,sect}$ and $S_{i,sect}$ are determined from [Geodesy data](#)

5.2.3. Tesselar Harmonics

These have the form:

$$U_{tesseral}(r, \phi_{gc}, \lambda) = \frac{\mu}{r} \sum_{i,j=2}^{\infty} (C_{i,j} \cos(i\lambda) + S_{i,j} \sin(i\lambda)) \left(\frac{R_e}{r}\right)^i P_{i,j}(\sin \phi_{gc}) \quad (33)$$



where, $C_{i,j}$ and $S_{i,j}$ are determined from Geodesy data

5.3. The J2 Perturbation

Many texts ignore the Sectorial and Tesseral Harmonics because the effect often appears random or hard to predict. Even in Zonal harmonics all harmonics, except first zonal harmonics, shall be ignored for simplicity.

$$\Delta U_{J2}(r, \phi_{gc}) = -\frac{\mu}{r} J_2 \left(\frac{R_e}{r}\right)^2 \left[\frac{3}{2} \sin^2(\phi_{gc}) - \frac{1}{2} \right] \quad (34)$$

where value of J_2 is 0.0010826. The above equation is expressed in ECI Frame. But to use our perturbation equations, we need a force expressed in the R-T-N frame.

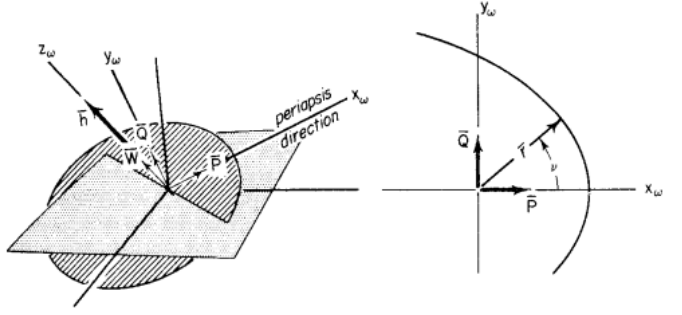
Since $\sin \Phi_{gc} = \frac{z}{r}$,

$$\Delta U_{J2}(r, \phi_{gc}) = -\frac{\mu}{r} \frac{J_2}{2} \left(\frac{R_e}{r}\right)^2 \left[\frac{3z^2}{r^2} - 1 \right] \quad (35)$$

The perturbation force is calculated as,

$$\begin{aligned} \vec{F} &= -\frac{\partial U_{J2}}{\partial r} \hat{e}_R + \frac{\partial U_{J2}}{\partial z} \hat{e}_z \\ &= -\mu J_2 R_e^2 \left[\frac{3z}{r^5} \hat{e}_z + \left(\frac{3}{2r^4} - \frac{15z^2}{2r^6} \right) \hat{e}_R \right] \end{aligned} \quad (36)$$

We need to write above equation in R-T-N frame. To convert a PQW vector to ECI, we use



$$\vec{r}_{ECI} = R_3(\Omega) R_1(i) R_3(\omega) \vec{r}_{PQW} = R_{PQW \rightarrow ECI} \vec{r}_{PQW} \quad (37)$$

$$R_{PQW \rightarrow ECI} = \begin{bmatrix} \cos \Omega & -\sin \Omega & 0 \\ \sin \Omega & \cos \Omega & 0 \\ 0 & 0 & 1 \end{bmatrix} \begin{bmatrix} 1 & 0 & 0 \\ 0 & \cos i & -\sin i \\ 0 & \sin i & \cos i \end{bmatrix} \begin{bmatrix} \cos \omega & -\sin \omega & 0 \\ \sin \omega & \cos \omega & 0 \\ 0 & 0 & 1 \end{bmatrix} \quad (38)$$

An additional rotation gives us the R-T-N frame,

$$R_{PQW \rightarrow ECI} = \begin{bmatrix} \cos \Omega & -\sin \Omega & 0 \\ \sin \Omega & \cos \Omega & 0 \\ 0 & 0 & 1 \end{bmatrix} \begin{bmatrix} 1 & 0 & 0 \\ 0 & \cos i & -\sin i \\ 0 & \sin i & \cos i \end{bmatrix} \begin{bmatrix} \cos(\omega + f) & -\sin(\omega + f) & 0 \\ \sin(\omega + f) & \cos(\omega + f) & 0 \\ 0 & 0 & 1 \end{bmatrix} \quad (39)$$

This gives us the expression,

$$\hat{e}_z = \sin i \sin(\omega + f) \hat{e}_R + \sin i \cos(\omega + f) \hat{e}_T + \cos i \hat{e}_N \quad (40)$$

Since $z = r \sin \phi_{gc} = r \sin i \sin(\omega + f)$. This yields the disturbing force in the R-T-N frame:

$$\vec{F} = -\frac{3\mu J_2 R_e^2}{r^4} \begin{bmatrix} \frac{1}{2} - \frac{3 \sin^2 i \sin^2 \theta}{2} \\ \sin^2 i \sin \theta \cos \theta \\ \sin i \sin \theta \cos i \end{bmatrix}_{RTN} \quad \text{where } \theta = \omega + f \quad (41)$$

$$N = -\frac{3\mu J_2 R_e^2}{r^4} \sin i \sin(\omega + f) \cos i \quad (42)$$

$$\dot{\Omega} = -\frac{3\mu J_2 R_e^2}{hp^3} \cos i \sin^2(\omega + f) [1 + e \cos f]^3 \quad (43)$$

...using $r = \frac{p}{1+e \cos f}$

$$\frac{d\Omega}{d\theta} = \frac{\dot{\Omega}}{\dot{\theta}} = \frac{\dot{\Omega}}{h/r^2} \quad (44)$$

Then the average change over an orbit is

$$\frac{d\Omega}{d\theta} \Big|_{AV} = \frac{1}{2\pi} \int_0^{2\pi} \frac{d\Omega}{d\theta} d\theta \Rightarrow \frac{d\Omega}{d\theta} \Big|_{AV} = -\frac{3}{2} J_2 \left(\frac{R_e}{p}\right)^2 \cos i \quad (45)$$

we can use the fact that $n = \frac{d\theta}{dt}$ to get the final expression:

$$\dot{\Omega}_{J_2,av} = -\frac{3}{2}nJ_2\left(\frac{R_e^2}{p}\right)\cos i \quad (46)$$

The above equation represents average change in RAAN over an orbit which is secular in nature.

J2 Nodal Regression: The ascending node migrates opposite the direction of flight. The equatorial bulge produces an extra pull in the equatorial plane which creates an averaged torque on the angular momentum vector. Like gravity, the torque causes \vec{h} to precess as shown in the figure below.

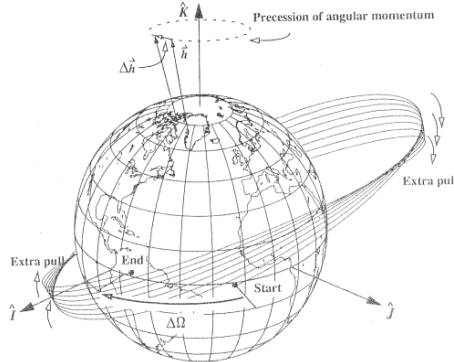


Fig-7: J2 Nodal Regression

For prograde orbit $\dot{\Omega}$ is *negative* whereas for retrograde orbit it is *positive*. Now recall the **Argument of Perigee** equation:

$$\dot{\omega} = -\Omega \cos i + \sqrt{\frac{a(1-e^2)}{e^2 \mu}} \left(-R \cos f + T \frac{(2+e \cos f) \sin f}{(a+e \cos f)} \right) \quad (47)$$

$$R = -\frac{3\mu J_2 R_e^2}{r^4} \left(\frac{1}{2} - \frac{3 \sin^2 i \sin^2 \theta}{2} \right)$$

$$T = -\frac{3\mu J_2 R_e^2}{r^4} (\sin^2 i \sin \theta \cos \theta) \quad (48)$$

The *argument of perigee* (ω) is linked to RAAN (Ω) as,

$$\frac{d\omega}{d\theta} = -\frac{d\Omega}{d\theta} \cos i + \frac{3J_2 R_e^2}{2p^2} \left[1 - \frac{3}{2} \sin^2 i \right] \quad (49)$$

$$\text{...where } \frac{d\Omega}{d\theta} \cos i = -\frac{3}{2} J_2 \left(\frac{R_e}{p} \right)^2 (1 - \sin^2 i)$$

$$\Rightarrow \dot{\omega}_{J_2,av} = \frac{3}{2} n J_2 \left(\frac{R_e^2}{p} \right)^2 \left[2 - \frac{5}{2} \sin^2 i \right] \quad (50)$$

Similar to nodal regression, but perigee moves forward or backward, depending on inclination.

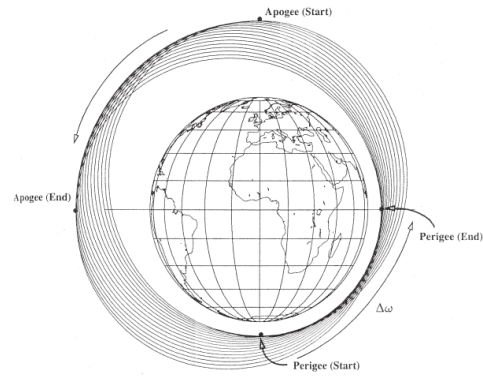


Fig-8: J2 Apsidal Rotation

5.4. J2 Effect

The J2 perturbation has significant effect on $\dot{\Omega}$ and $\dot{\omega}$. But its effect on other orbital elements is usually minor. For example, $\dot{a} \approx 0$.

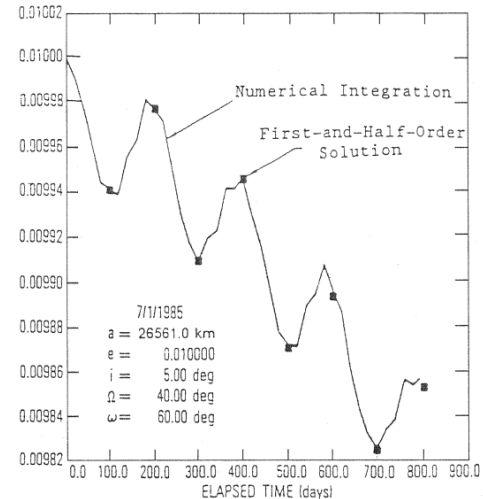


Fig-9: Eccentricity Change for Low-Inclination Orbit

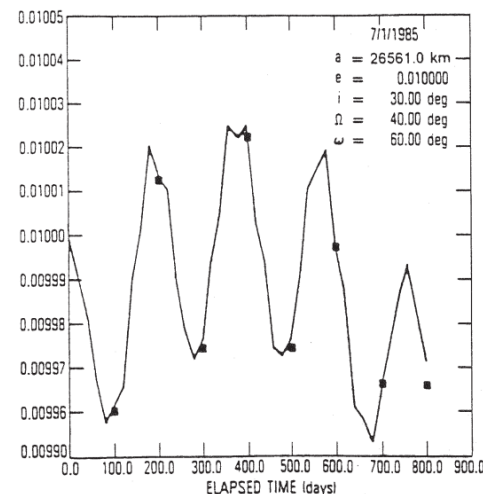


Fig-10: Eccentricity Change for Mid-Inclination Orbit

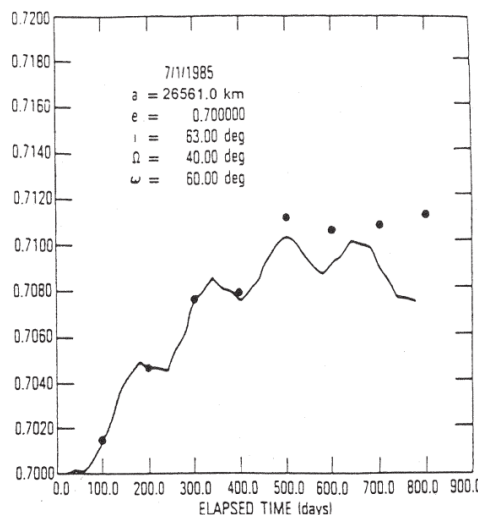


Fig-11: Eccentricity Change for High-Inclination Orbits

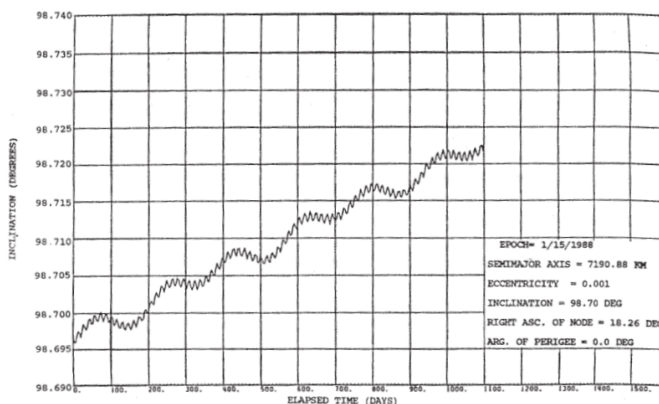


Fig-12: Inclination Change for Eccentric and Circular Orbits

5.5. J2 Special Orbits

Critically Inclined Orbit and *Sun-Synchronous Orbit* are two special orbits resulting due to J2 perturbations.

Critically Inclined Orbit: A Critically inclined orbit is the one where $\dot{\omega} = 0$. From the equation of $\dot{\omega}$,

$$4 - 5 \sin^2 i = 0 \Rightarrow i = \sin^{-1} \sqrt{\frac{4}{5}} = 63.43^\circ \text{ or } 116.57^\circ \quad (51)$$

Molniya Orbit and *Tundra Orbit* are examples of critically inclined orbits.

Sun-Synchronous Orbit: These are the orbits that maintain the same orientation of the orbital plane with respect to the sun. $\dot{\Omega}$ for a sun-synchronous orbit is $0.9855^\circ/\text{day}$ or $1.992 \times 10^{-7} \text{ rad/s}$.

6. Positive Perturbations

Even though perturbations, i.e. deviations from ideality are usually considered to be tough to work with, not all of its effects are considered "bad", or so to say. Some of its effects are pretty useful as well:

6.1. Lift and Slow Landing

Yes, the same drag that is responsible for perturbations in orbits of various rockets, space crafts and satellites can also produce lift, denoted by C_L , which can happen in the direction of e_R or even e_N ! Conventional designs such as that of a plane utilize this to keep the object in air.

But the most interesting aspect of it is the gradual re-entry of space crafts (a space-shuttle, for example) into the earth's atmosphere. Obviously, re-entry from such an altitude (400 km for the ISS) can spell havoc for the space craft due to the heat generated by air friction at such high velocities. To counter this, the vehicle's velocity must be reduced significantly. This is done using the atmosphere as a breaking mechanism which simultaneously also provides a decent amount of lift to the vehicle.

6.2. Debris Management

Although the expected lifetime of any satellite in the geosynchronous orbit is million of years, it is practically impossible for them to remain functioning for so long. Hence they are decommissioned and declared as space junk which could potentially prove harmful to other satellites in orbit. Hence, they need to be get rid of.

6.2.1. Graveyard Orbits

The energy required for the re-entry of a satellite into earth's atmosphere is approx. $\Delta V = 1500 \text{ m/s}$ which requires a ton of fuel. Hence it is impractical to do so. A much easier and less energy intensive way is to park it into one of the super-synchronous orbit, for example, the Graveyard Orbit, the maneuver from Geo-stationary orbit requires only a ΔV of about 11 m/s. This can be achieved via small perturbations to the orbit within a few months.

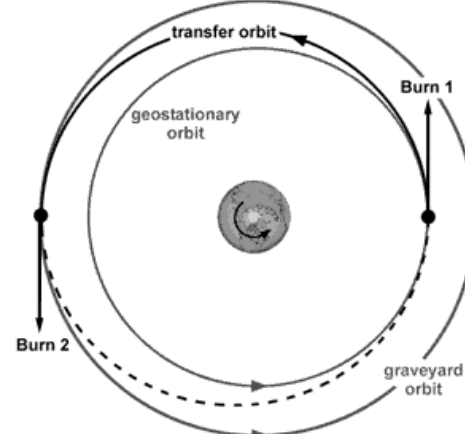


Fig-13: Achieving a Graveyard Orbit

6.2.2. Disposal Orbits

Another possible and more widely-accepted option is to move the satellite into disposal orbits. But this can be achieved only for satellites in LEO. Eventually, due to drag forces, they're able to slow down enough for their orbits to decay to a point where they are able to burn up in the upper atmosphere. This process can be typically finished within a year of end-of-life.

6.3. Lower ΔV requirement/ Gravity Assist

The most widely accepted measure of energy requirements to complete a maneuver in space is via its ΔV requirements, i.e. the velocity change it requires to reach to a particular point or orbit. Although using conventional trajectory, we can reduce this requirement, but to optimize it, we can use the presence of other heavenly bodies' gravitational forces to our benefit.

6.3.1. Using Lunar Gravity

Achieving a stable Low-Earth parking orbit requires significantly lower ΔV than direct transfer into GEO. Hence, it makes sense to first transfer the satellite/ payload into LEO before going higher up. In order to achieve GEO, or higher orbits, the gravitational pull of the moon can be exploited in order to reduce the potential energy barrier required to cross and move into a GEO.

6.3.2. Interplanetary Superhighway

A similar, but a little complicated maneuver can also be done for movement across the solar system. Using the gravitational forces exerted by the Gaseous Giants, especially Jupiter and Saturn, spacecraft can be propelled further with lower energy budget, often using gravitational turns. This phenomenon was used to send multiple space crafts such as Voyager 1, Voyager 2, Pioneer, etc to even leave the heliosphere! The optimum paths for lowest energy requirement made by the alignment of planets in our solar system, thus generates the Interplanetary Superhighway.

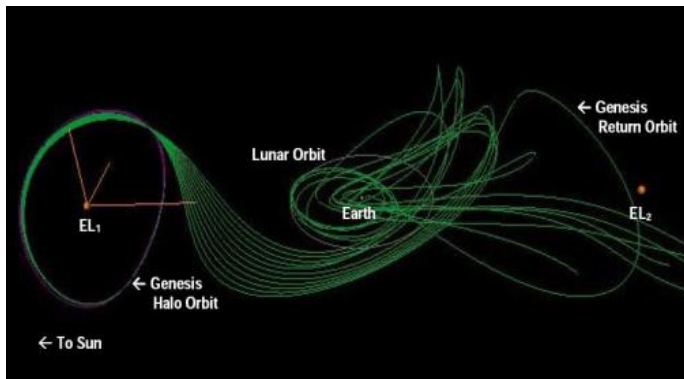


Fig-14: Interplanetary Superhighway

6.4. Asteroid Protection

Several rogue asteroids originating from the Kupier belt travel with incredible speeds which could spell havoc for us if they crashed into the earth.

6.4.1. Natural

For millions, if not, billions of years, the gaseous giants, especially Jupiter has protected earth from these type of impacts by slowly capturing the asteroids, over thousands of years into its stable Lagrange points - L4 and L5. These asteroids share the orbit of Jupiter usually forming what appears to a cloud at the Lagrange Points. They are also known as Trojans.

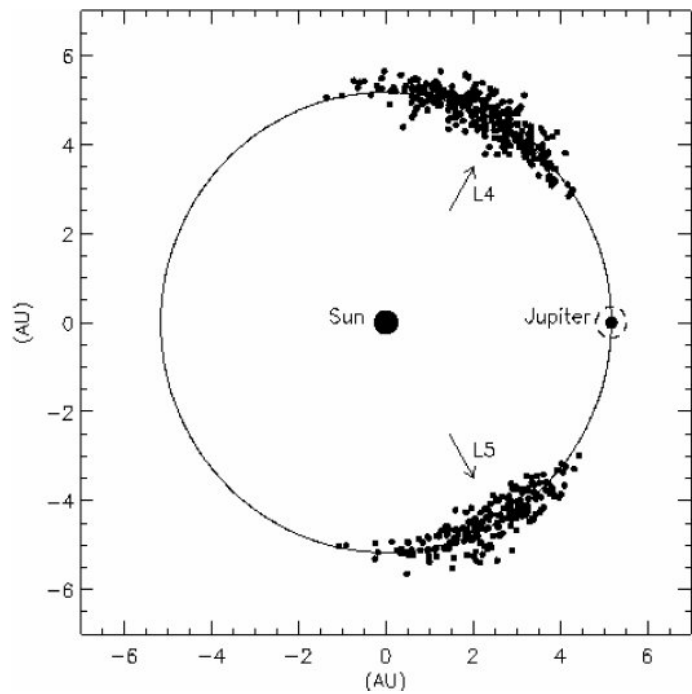


Fig-15: Jupiter's L4 and L5 points

6.4.2. Artificial

But as always, there are asteroids that Jupiter is unable to capture, especially the ones that possess weird orbital planes. The ones that have a potentiality to crash into earth in the near future are the most dangerous ones, for which, NASA has in place a planetary defense system for the NEOs (Near Earth Objects). If the due date of collision is far, the path of the object can be changed by applying carefully calculated impulses resulting in gradual but substantial change of the object's trajectory over the next few passes.

7. Newton's n-body problem

7.1. What it is?

While dealing with naturally occurring systems, it is hard, if not impossible to find a system consisting of only 2 bodies. We often encounter multiple celestial bodies interacting with each other, while remaining in a steady and stable orbit. Although we usually reduce it to a two body problem while solving for orbits, for example in the case of our solar system, consisting of 8 planets with a star at its center, it's much more difficult to ignore the effects of the remaining bodies in a system with comparable masses, take our nearest stellar neighbour, Proxima Centauri system. Consisting of 3 stars revolving around each other, the system is a perfect example of the 3-body problem.

7.2. Derivation of equations

While calculating the forces acting, trajectory and orbits of each and every system, it is advised to take into account the movement of the center of mass of the entire system. The position of the center of mass of a system with n masses can be calculated as:

$$\vec{r}_{cm} = \frac{\sum_{i=1}^n m_i \vec{r}_i}{\sum_{i=1}^n m_i} \quad (52)$$

Now, since no external force will be acting on it, the center of mass will remain stationary while the bodies move around it. Hence, on differentiation the above equation twice, we can equate the velocity and acceleration of the center of mass to 0, i.e.

$$\frac{d}{dt} \vec{r}_{cm} = \vec{v}_{cm} = 0, \quad \frac{d^2}{dt^2} \vec{r}_{cm} = \vec{a}_{cm} = 0 \quad (53)$$

Moreover, no external torque will be acting over the system. Hence, the angular momentum of the system about its center of mass will remain constant as well:

$$\sum_{i=1}^n m_i [\vec{r}_i - \vec{r}_{cm}] \times \vec{v}_i = 0 \quad (54)$$

As can be seen from the above equations, if we know the initial condition of the system, it is easy to predict the motion of each and every object in a 2-body system. However things start to get complicated if the no of objects involved are more than 2, resulting in beautiful systems. Our focus, for this project will be on the 3-body system.

7.3. 3-Body problem

Let us consider 3 bodies, namely m_1 , m_2 and m_3 , orbiting around each other. The gravitational force acting on each one of them can be written as:

$$m_i \ddot{r}_i = G \frac{m_i m_j}{r_{ij}} \hat{r}_{ij} + G \frac{m_i m_k}{r_{ik}} \hat{r}_{ik} \quad (55)$$

... where $i, j, k \in \{1, 2, 3\}$ and $i \neq j \neq k \neq i$

Now, since the 3 masses affect each other, the above forms a coupled system of equations, the solution of which is given by the partial differential equations:

$$\frac{d\vec{r}_i}{dt} = \frac{d\vec{T}}{d\vec{p}_i}, \quad \frac{d\vec{p}_i}{dt} = -\frac{d\vec{T}}{d\vec{r}_i}, \quad (56)$$

where

- T = total energy of the system = potential + kinetic
- p_i = momentum of the i^{th} body
- r_i = position of the i^{th} body

The above system of equations is non-integrable, hence, we're unable to find a general equation that can give us the trajectory of each of the bodies. This results in multiple possible periodic solutions, depending on the initial conditions, some of which are as follows, assuming equal masses of all 3 objects:

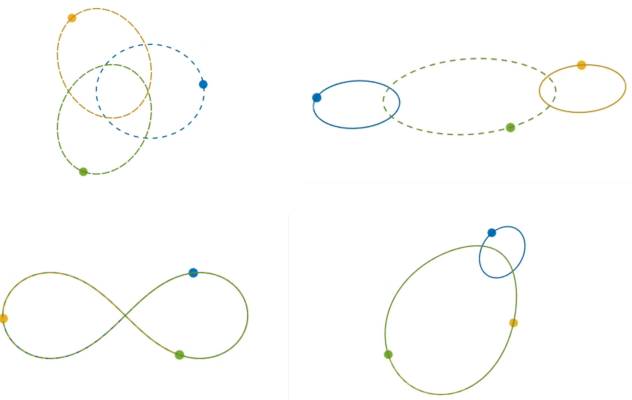
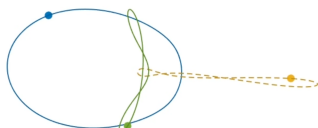


Fig-16: Possible stable periodic 3-body orbits

7.4. Chaos Theory

As to why the system of partial differential equations are non-integrable are due to the physical error that can be unintentionally induced. These errors can be due to multiple reasons, the primary one being observational.

As is always the case, observational error creep in resulting in results that are somewhat off. In this case, we cannot measure precisely the location or velocity of the planets or stars in question. Hence, the derived solution set will yield accurate answers initially but gradually over long time, say a few centuries, may not be quite right to accurately predict the motion of the celestial bodies.

Hence, over the years, these errors pile up resulting in a completely different orbits, caused by minuscule perturbations during each complete periodic motion. That's the practical application of butterfly effect, originating from chaos theory.

7.5. Lagrange Points

Now, if we take a stable periodic 3-body system, and reduce the mass of one of the bodies to 0 (or, tending to 0), we obtain some interesting results. It now effectively behaves as the conventional 2-body system.

The 0 mass object doesn't apply any force to the system, rather, if positioned correctly, can move in a periodic motion with the other two due to their gravitational forces equalling to the centripetal force required for the above motion. These selected points at which this phenomenon can occur are known as Lagrange points. Lagrange points exist for a general n-body system as well, but we'll limit ourselves to the Lagrange points of a 2-body system.

In a stable periodic 2-body system, there exist 5 Lagrange points. Of the five Lagrange points, three are unstable and two are stable. The unstable Lagrange points - labeled L1, L2 and L3 - lie along the line connecting the two large masses. The stable Lagrange points - labeled L4 and L5 - form the apex of two equilateral triangles that have the large masses at their vertices. L4 leads the orbit of earth and L5 follows.

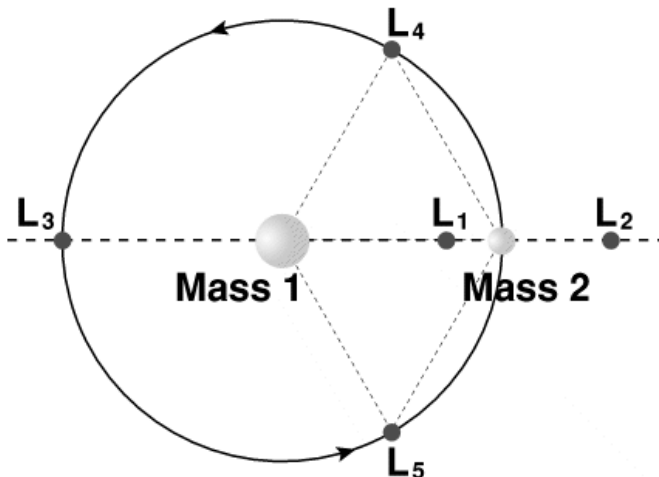


Fig-17: The five Lagrange points (Wikipedia)

8. Case Study: James Webb Space Telescope

8.1. Introduction

The highly awaited James Webb Space Telescope (JWST) was launched on December 25, 2021. Before diving into the details of its special orbit, let's get to know more about it.

The shape and design of the JWST are quite unique. Beneath, it has got an unusual five-layered tennis-court sized sun shield which is quite thin. The shield is made out of a material called "Kapton" and it basically helps to keep the telescope elements cold (the telescope operates at a temperature of about 50K) and away from heat radiations coming from the sun which may alter the efficiency of the telescope. The shield faces towards the sun.

The main aim behind maintaining such a low temperature at the telescope is connected to the kind of observations it would make. Unlike the Hubble Space Telescope, which majorly captured the light of the UV and visible region, the JWST would be majorly observing the infrared light, and thus other radiations coming from the sun would cause interference to it.

Infrared light, over the years, has helped uncover mysteries about a lot of distant galaxies and bodies which were millions of years old. It is believed that the JWST will further help us dive deep into ancient space.

8.2. Positioning at L2

Now comes another point to ponder upon, how is it ensured that the sun shield faces the sun at all times while orbiting? The answer to this is the special "Second Lagrange point", also called the L2 point, which is situated at a distance of about 1.5 million kilometres from the earth.

At the Lagrange points, as stated above, the gravitational pull of two large masses precisely equals the centripetal force required for a small object to move with them. In the case of JWST, the Sun and the Earth make the two large masses while the telescope represents the small object.

Why only L2? Because the location is ideal for astronomy as the telescope would be able to efficiently communicate with the Earth, and keep the Sun, Earth and Moon to one side to ensure solar power supply and provide a clear view of the deep space on the other side.

Note that L2 is a metastable point and thus, the telescope will drift away into an orbit around the Sun. The balance of the combined gravitational pull of the Sun and the Earth at the L2 point would ensure that JWST will keep up with the Earth as it goes around the Sun, which will keep it out of the shadows of both the Earth and the Moon, allowing it to operate 24x7. Thus, the amount of fuel spent on maintaining this orbit is also a bit less due to this reason.

8.3. Interesting Facts

In spite of this, the time span of the JWST would be very limited. It is expected that the mission would only be about 10 years long as eventually, the telescope would run out of fuel to support its orbit. This is unlike the Hubble Space Telescope which has been in service for about 30 years now. The large distance of the JWST from the Earth also makes it practically impossible to make any repairs at all in case anything goes wrong.

The grandness of the JWST can be understood by the fact that it would be about 100 times more powerful than the Hubble Space Telescope. The gold-plated mirror of JWST, when fully unfolded measures roughly 21 feet, much larger than that of Hubble (around 8 feet). Due to this large size, the mirrors had to be actually folded to be placed in the rocket's fairings and were designed keeping in mind the style of Japanese Origami.

Now, coming to the launch specifications of the telescope, Korou was chosen as the launch site due to its closeness to the equator which would actually provide an additional boost to the launch thanks to the spin of the earth. This is quite essential for a heavy telescope like the JWST, and for the same reason, the European Space Agency's Ariane 5 rocket was chosen, being one of the safest options available for heavy launches.

References

- [Orbital Mechanics](#), J. E. Prussing and B. A Conway
- [Dynamics and Control Algorithm for Low Earth Orbit Precision Formation Flying Satellites](#), Jesse Koovik Eyer
- [Spacecraft Control and Dynamics](#), Matthew M. Peet, Arizona State University
- [James Webb Space Telescope](#), Goddard Space Flight Center, NASA
- [Geodesy](#), National Geodetic Survey, NOAA
- [Intermediate Dynamics](#), Matt Sheen, Cornell University